



The Hsp90 inhibitor SNX-2112 induces apoptosis of human hepatocellular carcinoma cells: The role of ER stress



Xiao Wang^{a,b,1}, Shaoxiang Wang^{b,1}, Yuting Liu^b, Weichao Ding^b, Kai Zheng^b, Yangfei Xiang^b, Kaisheng Liu^b, Dongmei Wang^a, Yaoying Zeng^b, Min Xia^c, Depo Yang^{a,*}, Yifei Wang^{b,*}

^a School of Pharmaceutical Sciences, Sun Yat-sen University, Guangzhou, Guangdong, China

^b Guangzhou Jinan Biomedicine Research and Development Center, National Engineering Research Center of Genetic Medicine, Jinan University, Guangzhou, Guangdong, China

^c Guangzhou Tongde Pharmaceutical Co., Ltd, Guangzhou, Guangdong, China

ARTICLE INFO

Article history:

Received 8 February 2014

Available online 25 February 2014

Keywords:

Hsp90

SNX-2112

HCC

Apoptosis

ER stress

ABSTRACT

Heat shock protein 90 (Hsp90) has been predicted to be involved in hepatocellular carcinoma (HCC) therapy; however, the mechanisms of action remain elusive. SNX-2112 is an Hsp90 inhibitor showing broad antitumor activity. Here we aim to determine the role of the endoplasmic reticulum (ER) stress in SNX-2112-induced apoptosis in HCC cells. In general, three HCC cells (i.e., HepG2, Huh7, and SK-Hep1) were used in our experiments. The cell viability was determined by the CCK-8 assay. The apoptosis was analyzed using flow cytometry, laser scanning confocal microscopy (LSM) and Western blotting. The efficacy and mechanisms of action of SNX-2112 were also evaluated in a mouse xenograft model. We found that SNX-2112 showed stronger inhibition on cell growth than 17-AAG, a classical Hsp90 inhibitor. SNX-2112 treatment led to the caspase-dependent apoptosis. Interestingly, SNX-2112 decreased the expression levels of the ER chaperone proteins calnexin and immunoglobulin binding protein (BiP). It also inhibited all three ER stress sensors, namely, inositol-requiring gene 1 (IRE1), PKR-like ER kinase (PERK), and activating transcription factor 6 (ATF-6) *in vitro* and/or *in vivo*. However, the ER stress inducer tunicamycin strongly enhanced SNX-2112-induced apoptosis, whereas the IRE1 knockdown did not. Taken together, we for the first time indicated the possible apoptotic pathways of SNX-2112 in HCC cells, raising the possibility that the induction of ER stress might be favorable for SNX-2112-induced apoptosis.

© 2014 Elsevier Inc. All rights reserved.

1. Introduction

Heat shock protein 90 (Hsp90) is a crucial mediator of protein folding and stabilization, and of degradation of its client proteins [1]. The role of the Hsp90 in regulating cell proliferation and survival of tumor cells makes it an attractive therapeutic target. Inhibition of Hsp90 has been reported to induce apoptosis in multiple cancer cells. Hsp90 inhibitors can induce apoptosis through various pathways, such as mitochondria-mediated and death receptor-induced pathways [2–4].

Recently, several reports have shown that the endoplasmic reticulum (ER) stress-evoked pathway plays a role in apoptotic execution [5]. ER is a critical organelle for protein synthesis and folding, as well as cellular calcium storage [6]. ER stress results in accumulation of

unfolded or misfolded proteins and release of three sensors (PERK, IRE1, and ATF-6) from immunoglobulin binding protein (BiP), leading to the initiation of the unfolded protein response (UPR). If the stress is prolonged, or the UPR is unable to correct the balance, apoptotic cell death ensues [7,8]. However, whether and how this alternative pathway contributes to apoptosis induced by Hsp90 inhibitors is elusive.

Hsp90 is highly expressed in both HCC patients and cell lines [9,10], which suggests that Hsp90 inhibitors could be used to treat HCC. SNX-2112 is an Hsp90 inhibitor showing broad antitumor activity. Based on our previous studies [2,11,12], we hypothesized that the Hsp90 inhibitor SNX-2112 could induce HCC cells apoptosis. This study aimed to elucidate the possible mechanisms involved in SNX-2112-mediated apoptosis *in vitro* and *in vivo*. In addition to the two conventional pathways (mitochondria- and death receptor-mediated pathways), we have focused on the role of ER stress in SNX-2112-induced apoptosis.

* Corresponding authors. Fax: +86 20 85223426.

E-mail addresses: lssydp@mail.sysu.edu.cn (D. Yang), twang-yf@163.com (Y. Wang).

¹ These authors contributed equally to this work.

2. Material and methods

2.1. Reagents and anti-bodies

SNX-2112 was synthesized in our lab with a purity >98%, following the procedure previously described [13]. SNX-2112, 17-AAG (Alexis Biochemicals, San Diego, CA, USA), and tunicamycin (Sigma, St. Louis, MO, USA) were dissolved in dimethyl sulfoxide (DMSO, Sigma) at stock concentrations of 10 mM, 10 mM, and 10 mg/mL, respectively, and stored at -20°C .

Rabbit or mouse anti-human caspase-3, caspase-8, caspase-9, PARP, GAPDH, BiP, calnexin, PERK, and IRE1 α were purchased from Cell Signaling Technology (Beverly, MA, USA). Anti-ATF-6 α and horseradish peroxidase-conjugated secondary antibody were obtained from Santa Cruz Biotechnology (Santa Cruz, CA, USA).

2.2. Cell lines and cell culture

The normal human hepatocyte line HL-7702 and the human HCC cell lines: HepG2, Huh7, and SK-Hep1 (Cell Bank of the Chinese Academy of Sciences, Shanghai, China) were cultured in DMEM containing 10% FBS (fetal bovine serum, Hyclone, Logan, UT, USA) and 100 U/mL penicillin-streptomycin, and incubated at 37°C in an atmosphere of 5% CO_2 .

2.3. Cytotoxicity assay

The activities of SNX-2112 and 17-AAG against HepG2, Huh7, SK-Hep1 and HL-7702 cells were analyzed using a CCK-8 kit (Dojindo Laboratories, Kumamoto, Japan). Exponentially growing cells were seeded into 96-well culture plates ($5\text{--}10 \times 10^4$ cells/mL) in 100 μL medium and allowed to adhere overnight. HCC cells (HepG2, Huh7, and SK-Hep1) were treated with a series of concentrations (0–10 μM) of SNX-2112 or 17-AAG for 72 h. HL-7702 normal human cells were incubated with drugs at various concentrations (0–100 μM) for 72 h, along with an equal volume of DMSO as the solvent control.

After adding 10 μL CCK-8 solution per well, the plates were incubated at 37°C for 2 h. The absorbance was measured at 450 nm using a BioRad 680 microplate reader (BioRad, Hercules, CA, USA). Cell viability was calculated as (optical density of experimental sample/optical density of control) $\times 100\%$. The IC_{50} values were calculated using the PrismPad program.

2.4. Apoptosis evaluation

Morphological changes in the nuclear chromatin of HCC cells were detected by staining with 4'-6-diamidino-2-phenylindole (DAPI) purchased from Sigma (St. Louis, MO, USA). Cells were exposed to SNX-2112 for 48 h, or 0.25 $\mu\text{g/mL}$ tunicamycin plus SNX-2112 for 48 h. Then, cells were washed twice with ice-cold PBS, and fixed with 4% paraformaldehyde for 15 min at room temperature. Fixed cells were washed and stained with DAPI (5 $\mu\text{g/mL}$) for 10–15 min at 37°C . Cells were visualized by laser scanning confocal microscopy (LSM) using an LSM 510 (Zeiss, Oberkochen, Germany).

Apoptosis rates were calculated by measuring the sub-G1 DNA content. Cells were harvested, washed, and fixed with 70% ethanol overnight at 4°C , then, collected and resuspended in PBS containing 50 $\mu\text{g/mL}$ PI, 0.1 mg/mL RNase, and 0.2% Triton X-100 and incubated in the dark at 37°C for 30 min. Cells were determined on flow cytometry. All data were collected and analyzed by Becton Dickinson Cell Quest software.

2.5. Immunofluorescence staining

Cells were fixed, permeabilized on chambered coverslips, and blocked in PBS containing 5% bovine serum albumin (BSA) for 1 h, then incubated with calnexin antibody (1:100) for 1 h at room temperature. The cells were washed three times with PBS, and incubated with FITC-conjugated anti-rabbit IgG (1:1000) for 1 h. Cells were stained with DAPI and washed in PBS. Finally, the slides were mounted and examined by LSM.

2.6. Western blotting

Cells were harvested and lysed in radioimmuno-precipitation assay (RIPA) buffer (Beyotime, Shanghai, China) for 30 min on ice. After centrifugation at 13,000 rpm for 15 min, the supernatants were collected, and a BCA Protein Assay Kit (Beyotime, Shanghai, China) was used to evaluate protein concentrations of cell lysates. The lysates were mixed with $5 \times$ SDS buffer (Beyotime, Shanghai, China) and boiled for 10 min at 100°C . Equal amounts of protein lysates (30–50 μg) were resolved on 8–12% SDS-PAGE gels, transferred to PVDF membranes (Millipore, Boston, MA), and blocked in 5% skimmed milk for 1 h at room temperature.

The membranes were washed three times with Tris-buffered saline containing 0.1% Tween 20 (TBST), and then probed with the indicated antibodies overnight at 4°C . The membranes were washed three times with TBST, and then incubated with anti-rabbit or anti-mouse IgG (1:3000) for 1 h at room temperature. The protein bands were visualized using an enhanced ECL kit (chemiluminescence) (Beyotime, Shanghai, China), and imaged by autoradiography. GAPDH was used as the loading control.

2.7. Transfection

HepG2 and Huh7 cells were seeded in 96-well plates (8×10^3 cells per well) or in 6-well plates (1×10^5 cells per well) in antibiotic-free complete medium for 24 h. Cells were transfected with small interfering RNA (siRNA) targeted to human IRE1 (5'-GGACGUGAGCGACAGAAUATT-3' and 5'-UAUUCUGUCGUCACGUCCTG-3') or non-targeting siRNA (GenePharma, Shanghai, China) using Lipofectamin RNAiMAX (Invitrogen, Carlsbad, CA), according to the manufacturer's instructions. After 48 h, cells were treated with SNX-2112 (0.5 μM for HepG2 and 0.15 μM for Huh7 cells) for another 48 h. Cytotoxicity of the compound was determined by CCK-8 kit, and the percentages of apoptotic cells were analyzed by flow cytometry.

2.8. HCC xenograft experiments

Fifteen nu/nu athymic BALB/c male mice (4–6 weeks old) were obtained from the Experimental Animal Center of Sun Yat-sen University (Guangzhou, China). All animal experiments were performed in compliance with Institutional Animal Care and Use Committee guidelines. Tumors were established by flank injection of 5×10^6 cells suspended with reconstituted basement membrane (BD Biosciences, Bedford, MA) at a ratio of 2:1 (volume). When tumors reached 100 mm^3 , mice were randomly divided into two groups: control ($n = 7$) and SNX-2112 ($n = 8$). Animals were received alternate-day intraperitoneal injection of SNX-2112 (10 mg/kg) or an equal volume of diluents (10% DMSO) for 14 days. Tumor volumes were calculated using the formula: $1/2 \times \text{larger diameter} \times (\text{smaller diameter})^2$. Mice were sacrificed and tumors were excised and weighed. Tumor tissue was homogenized in a Dounce tissue grinder (Wheaton Instruments, Millville, NJ). Western blotting was used to determine the expression of PARP, BiP, IRE1 α and PERK.

2.9. Statistical analysis

The results are expressed as mean \pm SD of three independent experiments. Statistical analysis was performed using SPSS 18.0 for Windows (SPSS Inc., Chicago, IL, USA). Differences between two groups were analyzed using the two-tailed Student's *t*-test and groups of three or more were analyzed using one-way ANOVA with multiple comparisons. **P* < 0.05, ***P* < 0.01 were considered statistically significant in all experiments.

3. Results

3.1. SNX-2112-induced apoptosis was caspase-dependent and mediated via the mitochondrial and death receptor pathways

The effects of SNX-2112 on cell growth were determined using three types of HCC cells (HepG2, Huh7, and SK-Hep1) and a normal human hepatic cell line HL-7702. In HCC cells, SNX-2112 and 17-AAG (the positive control) significantly inhibited cell growth at 72 h (Fig. 1A). SNX-2112 inhibited cell viability dose-dependently with an IC₅₀ of 0.36 \pm 0.08 μ M in HepG2 cells, 0.12 \pm 0.02 μ M in Huh7 cells, and 0.24 \pm 0.04 μ M in SK-Hep1 cells. The calculated IC₅₀ values of 17-AAG were 0.53 \pm 0.09 μ M in HepG2 cells, 0.26 \pm 0.05 μ M in Huh7 cells, and 5.47 \pm 0.3 μ M in SK-Hep1 cells, respectively. This clearly indicated that SNX-2112 showed a greater inhibitory effect on cell growth than 17-AAG. Therefore, the IC₅₀ values of SNX-2112 were then chosen as the experimental concentrations (0.5 μ M, HepG2; 0.15 μ M, Huh7; 0.3 μ M, SK-Hep1). Meanwhile, in normal liver HL-7702 cells, treatment with SNX-2112 (100 μ M) resulted in a 30% decrease in cell viability, and we were unable to calculate the IC₅₀ value. The estimated IC₅₀ value of 17-AAG was 50.0 \pm 3.7 μ M (Supplementary Fig. 1). This suggested that SNX-2112 may be less toxic than 17-AAG.

To determine the effect of SNX-2112 on apoptosis, we examined the ability of SNX-2112 to induce the characteristic morphological changes of apoptosis using DAPI staining. Compared to the control group, SNX-2112-treated cells displayed apoptotic phenotypes, with signs of significant chromatin condensation and nuclear fragmentation (Fig. 1B). Flow cytometry results showed that SNX-2112 treatment led to accumulation of cells in the sub-G1 fraction for each cell line (Fig. 1C). In addition, we found that SNX-2112 treatment decreased the expression of three Hsp90 client proteins in a time-dependent manner, and it also led to a gradual increase of cells at G2/M phase (Supplementary Fig. 2).

The caspase enzymes catalyze specific cleavage of many key cellular proteins such as PARP (an indicator of apoptosis) [14]. SNX-2112 treatment increased the levels of cleaved caspase-3, caspase-8 (a downstream indicator of the death receptor apoptotic pathway), caspase-9 (a downstream indicator of the mitochondrial apoptotic pathway), and PARP (Fig. 1D). Furthermore, z-VAD-fmk (a pan-caspase inhibitor) prevented SNX-2112-induced apoptosis (Supplementary Fig. 3). Taken together, the results indicated that SNX-2112-induced apoptosis was caspase-dependent, and mediated by the death receptor and mitochondrial pathways.

3.2. SNX-2112 inhibited ER stress and UPR in vitro

To determine whether ER stress can be affected by SNX-2112, confocal immunofluorescence was used to detect the cellular localization and expression of the ER-localized molecular chaperone calnexin in HepG2 and Huh7 cells. SNX-2112 decreased the expression of calnexin (Fig. 2A), indicating that SNX-2112 might interfere with ER structure and/or function. Western blot results showed that treatment with SNX-2112 decreased the expression of calnexin and BiP in a time-dependent manner (Fig. 2B).

Furthermore, SNX-2112 treatment significantly decreased the levels of IRE1 α , PERK, and the cleaved form of ATF-6 α (Fig. 2C), which represent the three branches of UPR. Our findings suggested that SNX-2112 inhibited ER stress and inactivated the UPR in HCC cells.

3.3. SNX-2112 induced apoptosis and inhibited ER stress and UPR in vivo

The *in vivo* efficacy of SNX-2112 and mechanisms of action were determined in a mouse xenograft model. SNX-2112 treatment (14 days) produced an approximately 40% decrease in tumor weight (Fig. 3A). Treatment with SNX-2112 for 8 days led to a significant delay in tumor growth (Fig. 3B). The levels of cleaved PARP were significantly increased, indicating that apoptosis was induced *in vivo* (Fig. 3C). SNX-2112 exposure resulted in a significant decrease in protein levels of BiP, IRE1 α , and PERK in HCC xenograft tissues (Fig. 3D). These data clearly indicated that ER stress pathway might be involved in the antitumor effect of SNX-2112 *in vivo*, which support our *in vitro* studies.

3.4. SNX-2112-induced apoptosis was enhanced by the ER stress inducer tunicamycin

To further determine the contribution of ER stress in SNX-2112-induced apoptosis, the functionally validated siRNA against human IRE1 and the chemical inducer tunicamycin were used to interfere with ER stress pathway. The IRE1-specific siRNA markedly inhibited basal expression of IRE1 α in HepG2 and Huh7 cells (Fig. 4A). Transfection of IRE1 siRNA resulted in the attenuation of apoptosis induced by SNX-2112 (Fig. 4B). These results indicated that knock-down of IRE1 might be disadvantageous for SNX-2112-induced apoptosis.

Cells were pre-treated with tunicamycin for 6 h, then, incubated with SNX-2112 for another 48 h. 0.25 μ g/mL tunicamycin exhibited low cytotoxicity with <10% growth inhibition in HCC cells (Supplementary Fig. 4A) and enhanced the effect of various concentrations of SNX-2112 on HCC cell growth inhibition (Supplementary Fig. 4B). After exposure to 0.25 μ g/mL tunicamycin, the expression of BiP was markedly up-regulated. Use of tunicamycin up-regulated cleaved PARP (Fig. 4C), indicating that tunicamycin aggravated SNX-2112-induced apoptosis in HCC cells. It dramatically increased the sub-G1 apoptosis fraction from 38.52% to 68.36% (HepG2 cells) or 15.22% to 28.22% (Huh7 cells) (Fig. 4D). Our data consistently indicated that the induction of ER stress was favorable for SNX-2112-induced apoptosis.

4. Discussion

In this study we have determined the effects and mechanisms of Hsp90 inhibition on HCC cells using the synthetic functional inhibitor SNX-2112. Different from previous work, the focus of the present study is the role of ER stress in SNX-2112-induced apoptosis *in vitro* and *in vivo*. This study for the first time demonstrated that ER stress is an important factor to SNX-2112-induced apoptosis. We have provided four lines of evidence. First, morphological experiments showed that SNX-2112 treatment resulted in a decrease in the quantity of ER-localized molecular chaperone calnexin and BiP. Second, immunoblotting experiments showed that SNX-2112 decreased the protein levels of BiP, IRE1 α , and PERK *in vitro* and *in vivo*. Third, disruption of ER stress by specific IRE1 siRNA attenuated SNX-2112-mediated apoptosis. Fourth, use of the ER stress inducer tunicamycin enhanced SNX-2112-induced apoptosis.

We have shown that SNX-2112 inhibited ER stress and inactivated all three branches of UPR (i.e., IRE1 α , PERK, and ATF-6 α)

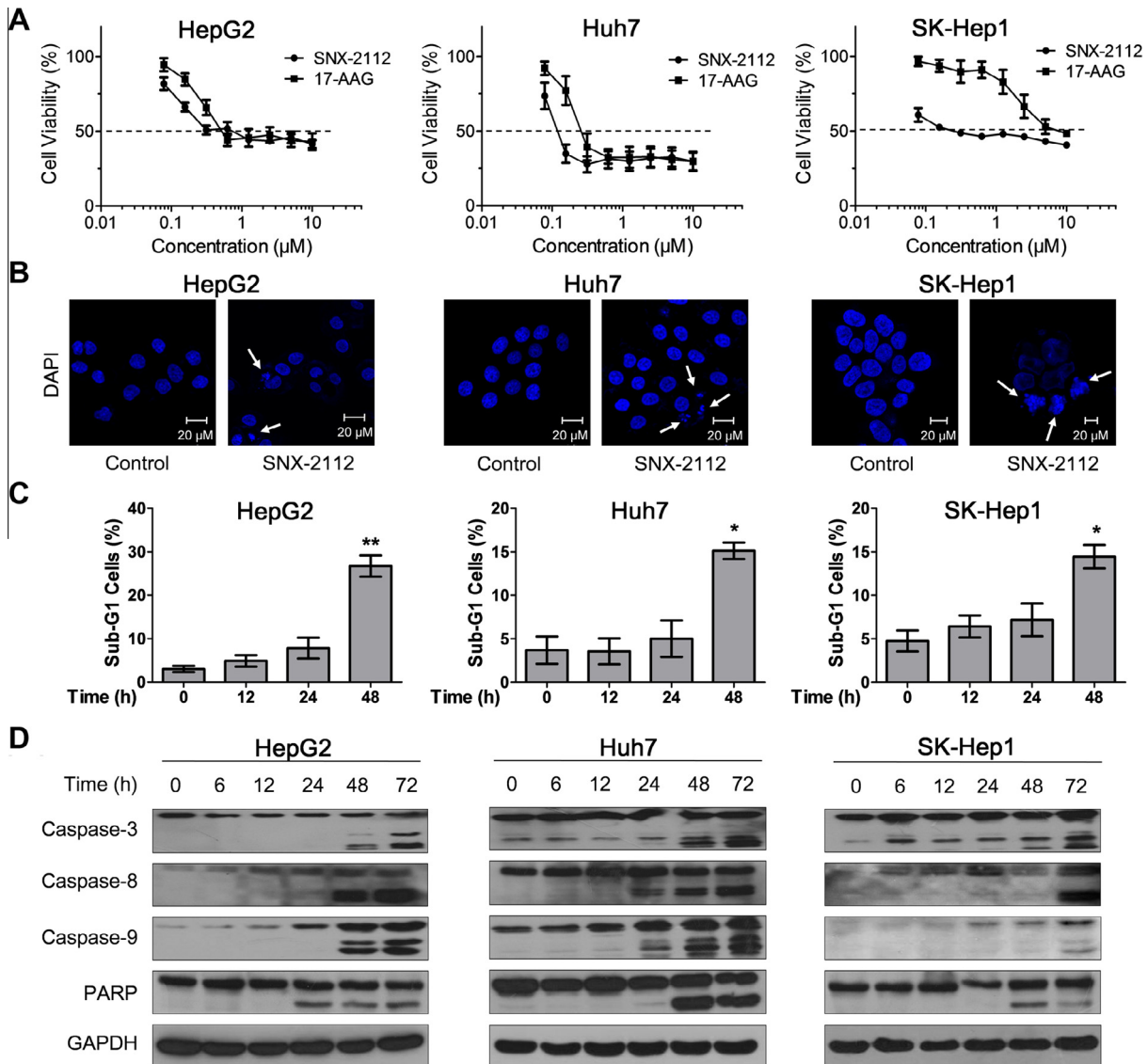


Fig. 1. SNX-2112-induced apoptosis depends on the activation of caspases in HCC cells. (A) The viability plots of HepG2, Huh7, and SK-Hep1 cells were determined by CCK-8 kit. The dashed lines indicate the IC₅₀ values of SNX-2112 in HCC cells. (B) Confocal images of DAPI-stained HepG2 cells, Huh7 cells, and SK-Hep1 cells (SNX-2112 treated; 0.5, 0.15, and 0.3 μM, respectively). White arrows indicate significant chromatin condensation and nuclear fragmentation. (C) The percentage of cells with sub-G1 DNA content was taken as a measure of apoptotic rate by flow cytometry. Statistical histograms indicate the percentage of cells in the sub-G1 phase. Data are mean ± SD (error bars) from three independent experiments (* $P < 0.05$; ** $P < 0.01$; compared with control). (D) The cleaved forms of caspase-3, caspase-8, caspase-9, and PARP were determined by Western blotting after exposure to SNX-2112 for the indicated times. GAPDH was used as a protein loading control.

in vitro and/or *in vivo*. Our result is consistent with the studies of Roue et al. and Patterson et al. [15,16], wherein IPI-504 (another type of Hsp90 inhibitor) similarly disrupted the UPR in mantle cell lymphoma and myeloma cells. The reason why use of an Hsp90 inhibitor could lead to suppression of UPR is probably because the three membrane-bound UPR sensors are Hsp90 client proteins [17,18]. However, the studies of Taiyab et al. and Davenport et al. revealed that inhibition of Hsp90 by GA and 17-AAG led to an increase of ER stress and up-regulation of the ER chaperones expression [19,20]. Therefore there is no general consensus on the regulation of ER stress by Hsp90 inhibitor. It is not yet clear why different types of Hsp90 inhibitors show distinct effects on ER stress and UPR.

Deciding whether to inhibit or promote ER stress for anti-cancer therapies requires careful analysis of mechanisms involved [21–23]. The ER stress signaling pathway is a complicated target for cancer therapy because of its dual role in cell survival and cell

death; therefore its potential benefit against tumor growth or regression remains controversial. We have demonstrated that the ER stress inducer tunicamycin enhanced SNX-2112-induced apoptosis, whereas the IRE1 knockdown did not. The finding that use of ER stress inducer is favorable for SNX-2112-induced apoptosis appears to be consistent with previous studies of Noda et al. and Nawrocki et al. [24,25]. In these studies, tunicamycin increased the sensitivity of various cancer cells to cisplatin or bortezomib-induced apoptosis.

It remains to be determined the underlying mechanisms of how tunicamycin enhances SNX-2112-induced apoptosis. Tunicamycin markedly up-regulates the expression of C/EBP homologous protein transcription factor (CHOP), an important pro-apoptotic element in ER stress-induced apoptosis [26,27]. Use of tunicamycin also induces activation of c-Jun NH2-terminal kinase (JNK) pathway, which is known to influence the cell death machinery through the regulation of Bcl-2 family proteins [25,28]. Therefore, on the

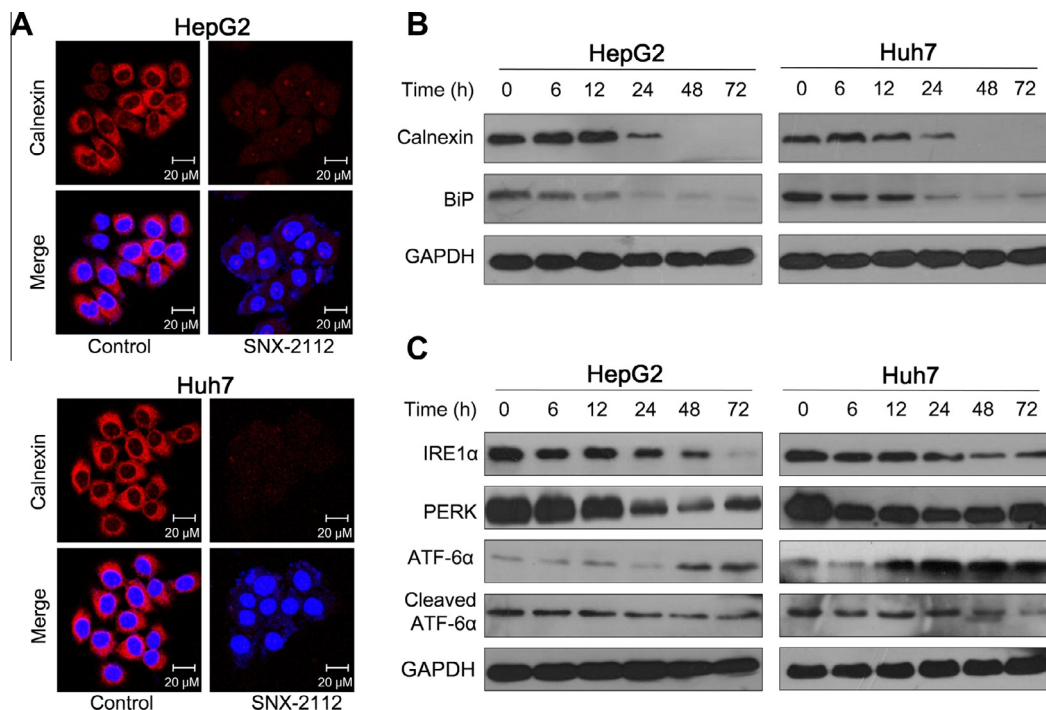


Fig. 2. SNX-2112 inhibits ER stress and inactivates the UPR *in vitro*. (A) The location and expression level of calnexin (Red) in HepG2 and Huh7 cells after incubating with 0.5 μ M (HepG2) or 0.15 μ M (Huh7) SNX-2112 for 48 h. (B) Western blots of the expression levels of calnexin and BiP after treatment with SNX-2112 for the indicated times. (C) Western blotting time course analyses show expression of the three UPR sensors: PERK, IRE1 α , and ATF-6 α in HepG2 and Huh7 cells after exposure to SNX-2112.

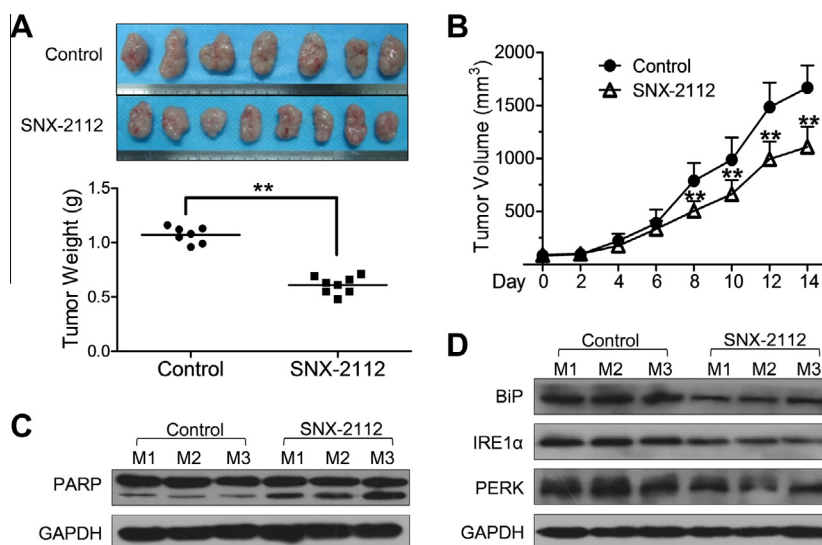


Fig. 3. SNX-2112 inhibits liver cancer growth, induces apoptosis, and inactivates the UPR in HCC xenograft model. (A) SNX-2112 reduced tumor burden. Pictures of Huh7 xenografts tumor tissue excised from nude mice after euthanization (upper panels). Lower panel is a scatter plot of the weight of each tumor from individual mice. (B) Treatment with SNX-2112 inhibited tumor growth in Huh7 xenograft models. (C, D) Western blot results for PARP, BiP, IRE1 α , PERK, and GAPDH in Huh7 xenografts. Data are mean \pm SD. ** P < 0.01; compared with control group.

basis of the literature, it is speculated that aggravation of apoptosis by tunicamycin is mediated through CHOP and JNK pathway.

In conclusion, we have demonstrated that mitochondrial-, death receptor-, and ER stress-provoked pathways were involved in SNX-2112-induced apoptosis in HCC cells. The ER stress inducer tunicamycin strongly enhanced SNX-2112-induced apoptosis, whereas the IRE1 knockdown did not. These findings indicate that ER stress inducers may be used as adjuvant to SNX-2112 chemotherapy for the purpose of efficacy enhancement. Our study

provides a mechanistic insight into how SNX-2112 leads to apoptosis, and establishes a possible connection between ER stress and SNX-2112-induced apoptosis.

Conflict of interest

The authors have no conflict of interests to declare.

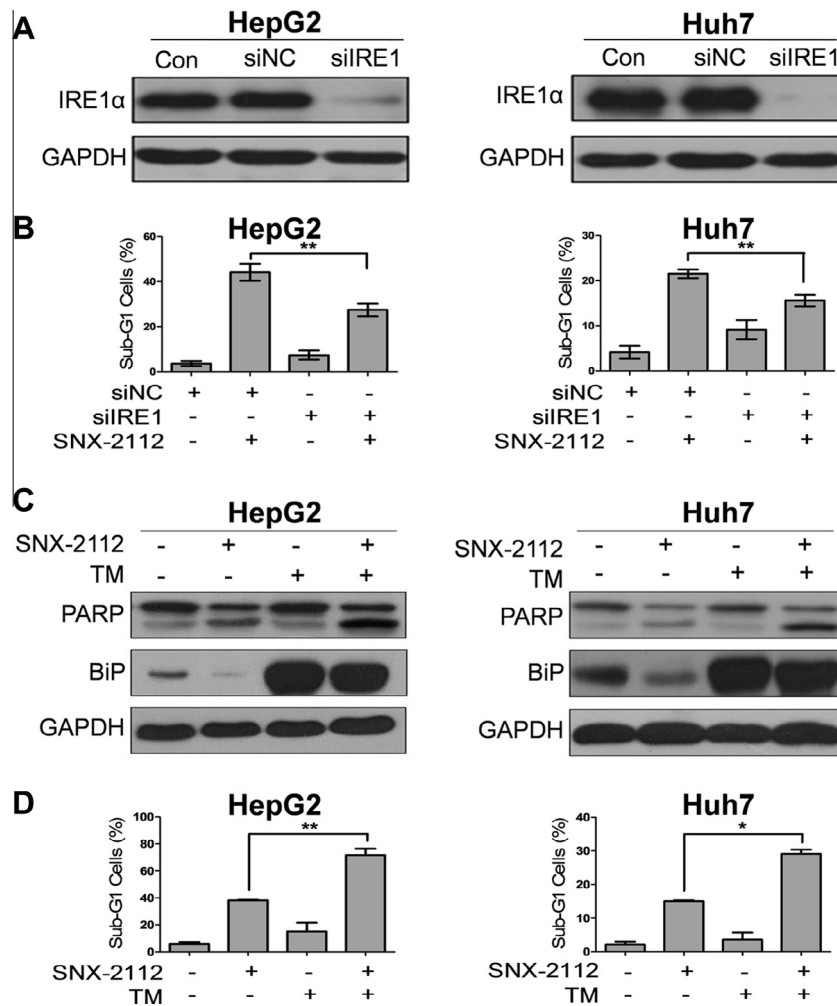


Fig. 4. SNX-2112-induced apoptosis is enhanced by the ER stress inducer tunicamycin. HepG2 and Huh7 cells were transfected with IRE1 or non-targeting siRNA (siNC) for 48 h. (A) The immunoblot confirms knockdown. (B) Transfected HepG2 and Huh7 cells were cultured for 48 h with or without SNX-2112 (SNX). Cell apoptosis was calculated by flow cytometry. $^*P < 0.05$; $^{**}P < 0.01$; siIRE1 + SNX versus siNC + SNX. siIRE1, IRE1 siRNA. (C) Western blotting was done on HCC cells lysates treated with SNX-2112, tunicamycin (TM), and the combination for 48 h using the PARP and BiP antibodies. GAPDH was used as the protein loading control. (D) After exposure to SNX-2112 plus TM for 48 h, cell apoptosis was calculated by flow cytometry. Data are the mean \pm SD ($n = 3$, $^*P < 0.05$; $^{**}P < 0.01$; SNX-2112 versus SNX-2112 + TM).

Acknowledgments

We thank Prof. Bao-Jian Wu from Jinan University (Guangzhou, China) for proofreading the manuscript. We thank Genepharma Co., Ltd., for the synthesis of siRNAs.

This work was supported by Grants from the National Natural Science Foundation of China (Grant 81201727), the China Postdoctoral Science Foundation (Grants 2012M511882, 2013T60827), the open project of State Key Laboratory of Molecular Oncology (SKL-KF-2013-14), Guangdong Province and Ministry of Education Ministry of Science and Technology Products Research Combined Platform Project (Grant 2010B091000013), the Major Platform Project Funds of Administration of Ocean and Fisheries of Guangdong, China (GD2012-D01-002), and the Natural Science Foundation of Guangdong Province (Grant S2012040006873).

Appendix A. Supplementary data

Supplementary data associated with this article can be found, in the online version, at <http://dx.doi.org/10.1016/j.bbrc.2014.02.081>.

References

- [1] M.P. Goetz, D.O. Toft, M.M. Ames, et al., The Hsp90 chaperone complex as a novel target for cancer therapy, *Ann. Oncol.* 14 (2003) 1169–1176.
- [2] K.S. Liu, H. Liu, J.H. Qi, et al., SNX-2112, an Hsp90 inhibitor, induces apoptosis and autophagy via degradation of Hsp90 client proteins in human melanoma A-375 cells, *Cancer Lett.* 318 (2012) 180–188.
- [3] M.D. Siegelin, A. Habel, T. Gaiser, 17-AAG sensitized malignant glioma cells to death-receptor mediated apoptosis, *Neurobiol. Dis.* 33 (2009) 243–249.
- [4] C. Gallerne, A. Prola, C. Lemaire, Hsp90 inhibition by PU-H71 induces apoptosis through endoplasmic reticulum stress and mitochondrial pathway in cancer cells and overcomes the resistance conferred by Bcl-2, *Biochim. Biophys. Acta* 2013 (1833) 1356–1366.
- [5] A.M. Gorman, S.J. Healy, R. Jager, et al., Stress management at the ER: regulators of ER stress-induced apoptosis, *Pharmacol. Ther.* 134 (2012) 306–316.
- [6] W. Paschen, Dependence of vital cell function on endoplasmic reticulum calcium levels: implications for the mechanisms underlying neuronal cell injury in different pathological states, *Cell Calcium* 29 (2001) 1–11.
- [7] S. Bernales, F.R. Papa, P. Walter, Intracellular signaling by the unfolded protein response, *Annu. Rev. Cell Dev. Biol.* 22 (2006) 487–508.
- [8] P. Walter, D. Ron, The unfolded protein response: from stress pathway to homeostatic regulation, *Science* 334 (2011) 1081–1086.
- [9] R.M. Pascale, M.M. Simile, D.F. Calvisi, et al., Role of HSP90, CDC37, and CRM1 as modulators of P16(INK4A) activity in rat liver carcinogenesis and human liver cancer, *Hepatology* 42 (2005) 1310–1319.
- [10] C.L. Lee, H.H. Hsiao, C.W. Lin, et al., Strategic shotgun proteomics approach for efficient construction of an expression map of targeted protein families in hepatoma cell lines, *Proteomics* 3 (2003) 2472–2486.
- [11] L. Jin, C.L. Xiao, C.H. Lu, et al., Transcriptomic and proteomic approach to studying SNX-2112-induced K562 cells apoptosis and anti-leukemia activity in K562-NOD/SCID mice, *FEBS Lett.* 583 (2009) 1859–1866.
- [12] S.X. Wang, H.Q. Ju, K.S. Liu, et al., SNX-2112, a novel Hsp90 inhibitor, induces G2/M cell cycle arrest and apoptosis in MCF-7 cells, *Biosci. Biotechnol. Biochem.* 75 (2011) 1540–1545.

- [13] T.E. Barta, J.M. Veal, J.W. Rice, et al., Discovery of benzamide tetrahydro-4H-carbazol-4-ones as novel small molecule inhibitors of Hsp90, *Bioorg. Med. Chem. Lett.* 18 (2008) 3517–3521.
- [14] B.B. Wolf, D.R. Green, Suicidal tendencies: apoptotic cell death by caspase family proteinases, *J. Biol. Chem.* 274 (1999) 20049–20052.
- [15] G. Roue, P. Perez-Galan, A. Mozos, et al., The Hsp90 inhibitor IPI-504 overcomes bortezomib resistance in mantle cell lymphoma in vitro and in vivo by down-regulation of the prosurvival ER chaperone BiP/Grp78, *Blood* 117 (2011) 1270–1279.
- [16] J. Patterson, V.J. Palombella, C. Fritz, et al., IPI-504, a novel and soluble HSP-90 inhibitor, blocks the unfolded protein response in multiple myeloma cells, *Cancer Chemother. Pharmacol.* 61 (2008) 923–932.
- [17] M.G. Marcu, M. Doyle, A. Bertolotti, et al., Heat shock protein 90 modulates the unfolded protein response by stabilizing IRE1 α , *Mol. Cell. Biol.* 22 (2002) 8506–8513.
- [18] T.S. Kim, C.Y. Jang, H.D. Kim, et al., Interaction of Hsp90 with ribosomal proteins protects from ubiquitination and proteasome-dependent degradation, *Mol. Biol. Cell* 17 (2006) 824–833.
- [19] A. Taiyab, A.S. Sreedhar, M. Rao, Ch, Hsp90 inhibitors, GA and 17AAG, lead to ER stress-induced apoptosis in rat histiocytoma, *Biochem. Pharmacol.* 78 (2009) 142–152.
- [20] E.L. Davenport, H.E. Moore, A.S. Dunlop, et al., Heat shock protein inhibition is associated with activation of the unfolded protein response pathway in myeloma plasma cells, *Blood* 110 (2007) 2641–2649.
- [21] D.G. Breckenridge, M. Germain, J.P. Mathai, et al., Regulation of apoptosis by endoplasmic reticulum pathways, *Oncogene* 22 (2003) 8608–8618.
- [22] C. Xu, B. Bailly-Maitre, J.C. Reed, Endoplasmic reticulum stress: cell life and death decisions, *J. Clin. Invest.* 115 (2005) 2656–2664.
- [23] T. Verfaillie, A.D. Garg, P. Agostinis, Targeting ER stress induced apoptosis and inflammation in cancer, *Cancer Lett.* 332 (2013) 249–264.
- [24] I. Noda, S. Fujieda, M. Seki, et al., Inhibition of N-linked glycosylation by tunicamycin enhances sensitivity to cisplatin in human head-and-neck carcinoma cells, *Int. J. Cancer* 80 (1999) 279–284.
- [25] S.T. Nawrocki, J.S. Carew, K. Dunner Jr, et al., Bortezomib inhibits PKR-like endoplasmic reticulum (ER) kinase and induces apoptosis via ER stress in human pancreatic cancer cells, *Cancer Res.* 65 (2005) 11510–11519.
- [26] P.T. Huong, D.O. Moon, S.O. Kim, et al., Proteasome inhibitor-I enhances tunicamycin-induced chemosensitization of prostate cancer cells through regulation of NF-kappaB and CHOP expression, *Cell. Signal.* 23 (2011) 857–865.
- [27] T. Shiraishi, T. Yoshida, S. Nakata, et al., Tunicamycin enhances tumor necrosis factor-related apoptosis-inducing ligand-induced apoptosis in human prostate cancer cells, *Cancer Res.* 65 (2005) 6364–6370.
- [28] H. Puthalakath, L.A. O'Reilly, P. Gunn, et al., ER stress triggers apoptosis by activating BH3-only protein Bim, *Cell* 129 (2007) 1337–1349.